Hindawi
Shock and Vibration
Volume 2019, Article ID 7806015, 13 pages
https://doi.org/10.1155/2019/7806015

Research Article

CEEMDAN-Based Permutation Entropy: A Suitable Feature for the Fault Identification of Spiral-Bevel Gears

Lingli Jiang,[1,2] Hongchuang Tan,[2] Xuejun Li,[1,2] Liman Chen,[2] and Dalian Yang[2]

[1]*School of Mechanical & Electrical Engineering, Foshan University, Foshan 528000, China*
[2]*Hunan Provincial Key Laboratory of Health Maintenance for Mechanical Equipment, Hunan University of Science and Technology, Xiangtan, Hunan 411201, China*

Correspondence should be addressed to Xuejun Li; hnkjdxlxj@163.com

Received 26 July 2019; Revised 26 September 2019; Accepted 22 October 2019; Published 2 December 2019

Guest Editor: Franco Concli

A spiral-bevel gear is a basic transmission component and is widely used in mechanical equipment; thus, it is important to monitor and diagnose its running state to ensure safe operation of the entire equipment setup. The vibration signals of spiral-bevel gears are typically quite complicated, as they present both nonlinear and nonstationary characteristics and are interfered with by strong noise. The complete ensemble empirical mode decomposition with adaptive noise (CEEMDAN) method has been proven to be an effective method for analyzing this kind of signal. However, the fault feature information after CEEMDAN is not obvious and needs to be quantified. Permutation entropy can be used to quantify the randomness, complexity, and mutation of vibration time-series signals. This paper proposes to take the CEEMDAN-based permutation entropy as the sensitive feature for spiral-bevel gear fault identification. First, the raw vibration signal is decomposed by the CEEMDAN method to obtain a series of intrinsic modal functions (IMFs). The IMFs which included greater amounts fault information are selected as the optimal IMFs based on the correlation coefficient. Next, the permutation entropy values of the optimal IMFs are calculated. In order to obtain accurate permutation entropy values, the two key parameters, namely, embedding dimension and delay time, are optimized by using the overlapping parameter method. In order to assess the sensibility of the permutation entropy features, the support vector machine (SVM) is used as the classifier for fault mode identification, and the diagnostic accuracy can verify its sensibility. The permutation entropy of CEEMDAN-based/EEMD-based/EMD-based features, combined with SVM, is applied to identify three different fault modes of spiral-bevel gears. Their respective diagnostic accuracies are 100%, 88.33%, and 83.33%, which indicate that the CEEMDAN-based permutation entropy is the most sensitive feature for the fault identification of spiral-bevel gears.

1. Introduction

Spiral-bevel gear transmission is a transmission method commonly used in mechanical equipment, which has the advantages of large overlap coefficient, strong carrying capacity, high transmission ratio, smooth transmission, low noise, etc., and is widely used in aviation, automobile, mining, and other fields. In the transmission process, as spiral-bevel gears are affected by manufacturing errors and installation errors, poor lubrication, excessive speed, and overload working conditions, they are prone to damage and failure. This results in abnormal vibration, which will affect the normal operation of the entire transmission system and even the entire mechanical equipment setup, thus leading to safety accidents and causing significant economic losses. Therefore, the monitoring and diagnosis of the running state of spiral-bevel gears can ensure that the entire transmission system operates safely, efficiently, and reposefully, which has important practical significance. The vibration signal of spiral-bevel gears is extremely complex, as it is affected by the constant change of meshing logarithm, meshing point position, and instantaneous transmission ratio. In particular, as failure occurs, the signal exhibits strong

nonlinear and nonstationary characteristics and is interfered with by strong noise. Fault characteristic information is submerged in strong noise, which is difficult to identify [1, 2]. At present, some researchers are interested in the typical fault diagnosis of spiral-bevel gears [3–5], which mainly focuses on the feature extraction based on wavelet decomposition, such as the discrete wavelet-based method for the fault diagnosis of arc tooth wimble gears [4] and adaptive multiwavelet-based method for the fault diagnosis of spiral-bevel gears [5]. Generally speaking, compared with the parallel shaft gear system and planetary gear system, research on the fault diagnosis of spiral-bevel gear systems is insufficient [6, 7].

Signal processing methods have been developed rapidly in recent years. The traditional signal processing method is based on Fourier transform, but this method cannot obtain the time-domain- and frequency-domain-analyzed results simultaneously. For nonlinear and nonstationary vibration signals, important feature information is embedded in the time-frequency domain, so the time-domain- and frequency-domain-analyzed results need to be displayed at the same time. To effectively extract the fault features from the nonlinear and nonstationary vibration signals, many time-frequency analysis methods have been applied to fault diagnoses for vibration signal decomposition, such as short-time Fourier transform (STFT), Wigner–Ville distribution (WVD), wavelet decomposition (WD), empirical mode decomposition (EMD), and so on [8]. Empirical mode decomposition (EMD) is one of the most powerful signal processing techniques that can be used and have been extensively studied and widely applied in fault diagnosis [9]. EMD is based on the local characteristic timescales of a signal and can decompose the signal into a set of complete and almost orthogonal components known as intrinsic mode function (IMF). The IMFs indicate the natural oscillatory mode imbedded in the signal and serve as the basis functions, which are determined by the signal itself, rather than by predetermined kernels. Therefore, it is a self-adaptive signal processing technique that is suitable for nonlinear and nonstationary processes and is suitable for fault feature extraction of spiral-bevel gears [9, 10]. However, EMD has a major drawback, namely, the frequent appearance of mode mixing, which signifies that a single IMF consists of either signals of widely disparate scales, or a signal of a similar scale residing in different IMF components. In order to reduce this drawback of EMD, Wu and Huang proposed the ensemble empirical mode decomposition (EEMD) method based on EMD, which defines the true IMF components as the mean of an ensemble of trials, each consisting of the signal plus a white noise of finite amplitude [11]. The added white noise would populate the whole time-frequency space uniformly with the constituting components of different scales. When the signal is added to this uniformly distributed white background, the bits of signal of different scales are automatically projected onto proper scales of reference established by the white noise in the background. Undoubtedly, EEMD is a breakthrough in the development of EMD algorithm and works well to enhance the stability of EMD algorithm remarkably. Practicality, however, limits the number that one could employ in the ensemble; therefore, the resulting IMFs derived from EEMD would inevitably be contaminated by the added noise, especially when the number of ensembles is relatively low. In light of this problem, Yeh and Huang proposed a novel noise enhanced algorithm to improve the efficiency of the original noise-assisted algorithm of EEMD, by using each noise in pairs with plus and minus signs. Contrary to the requirements of EEMD, which call for independent and identically distributed noise, the present paired noises are perfectly anticorrelated. The advantage of this approach, however, is to have an exact cancellation of the residual noise in the reconstruction of the signal, which is known as complementary ensemble empirical mode decomposition (CEEMD) [12]. Furthermore, Torres proposed a noise-enhanced data analysis method known as complete ensemble empirical mode decomposition with adaptive noise (CEEMDAN), in which the residue of added white noises can be extracted from the mixtures of data and white noise via pairs of complementary ensemble IMFs with positive and negative added white noise [13]. CEEMDAN is the development of the EMD, EEMD, and CEEMD, which is more effective in terms of decomposition ability and can effectively reduce the residual noise in the reconstructed signal. Until now, scholars have studied CEEMDAN and achieved good results [14, 15]. Therefore, this paper chooses CEEMDAN to decompose the vibration signals of the spiral-bevel gears in different fault states, and the raw signal is decomposed into a series of IMFs. In order to reduce the amount of calculation, the IMFs including relatively large amounts of fault information are selected as the optimal IMFs based on the correlation coefficient.

The fault information in the optimal IMFs is not obvious and must be quantified. Using the quantified value of energy, entropy and energy entropy as a typical fault sensitive feature is very popular in the fault diagnosis domain [16–18]. Along with the development of entropy theory, permutation entropy (PE) has been proposed [19]. Compared with other entropy theories, permutation entropy is characterized by less computation and strong robustness, which can be used to detect the randomness, complexity, and mutation time-series signal [20, 21]. It can be used to quantify the fault features of mechanical vibration signals and has been preliminarily applied in mechanical fault diagnosis. For example, Ding et al. [22] studied the difference of permutation entropy among three states of a planetary gearbox and proposed the fault diagnosis method of the planetary gearbox based on the permutation entropy of local mean decomposition. Zheng et al. [23] proposed the multiscale permutation entropy to quantify the fault features of the bearing signal. When the spiral-bevel gear is running under fault conditions, its vibration signal is complex and changeable, and the permutation entropy can reflect the rule embedded in the vibration signal.

Therefore, in the present paper, CEEMDAN-based permutation entropy is used as the fault sensitive feature for spiral-bevel gear fault state recognition. In the calculation process of permutation entropy, the different parameter settings have a great impact on the calculation results. The optimized parameters of embedding dimension and time delay are also studied in this paper.

After the raw vibration signal is decomposed by CEEMDAN and a series of intrinsic modal functions (IMF) is obtained, the permutation entropy of the optimal IMFs is quantified. With this, the fault feature of spiral-bevel gears is extracted. In order to assess the sensibility of the permutation entropy features, the support vector machine (SVM) is used as the classifier for fault mode identification, and the diagnostic accuracy can verify its sensibility. The permutation entropy of CEEMDAN-based features is applied to identify three different fault modes of spiral-bevel gears, and these are then compared with the permutation entropy of EMD-based and EEMD-based features. This paper is structured as follows. Section 2 states the feature extraction and its sensibility assessment procedure. Section 3 presents experiments for the vibration signal of the acquisition of spiral-bevel gears. Section 4 presents the experiment analysis. Section 5 proposes the conclusion of this paper.

2. Theoretical Frameworks

2.1. CEEMDAN and Selection of IMFs

2.1.1. CEEMDAN Theory. To better describe the CEEMDAN algorithm, we define an operator $E_k(\cdot)$, the function of which is to solve the kth modal component IMF_k of the EMD decomposition. w^i is the white noise satisfying the distribution of $N(0,1)$, and ε_k is the amplitude coefficient of white noise added for the Kth time. The decomposition process for CEEMDAN is as follows:

(1) The white noise $X(t)+\varepsilon_0 w^i(t)$ is added to the original signal, and Ith EMD decomposition is performed. Then, the average operation is performed on the result to obtain IMF1:

$$\mathrm{IMF}_1 = \frac{1}{I}\sum_{i=1}^{I} E_1\left(X(t)+\varepsilon_0 w^i(t)\right). \tag{1}$$

(2) The first-stage residual component can then be calculated:

$$r_1(t) = X(t) - \mathrm{IMF}_1. \tag{2}$$

The white noise $r_1(t)+\varepsilon_1 E_1(\omega^i(t))$, $i=1,2,\ldots,I$ is added to the first-stage residual component, and the EMD is performed. Then, IMF_2 can be calculated using the mean value of the first IMF:

$$\mathrm{IMF}_2 = \frac{1}{I}\sum_{i=1}^{I} E_1\left(r_1(t)+\varepsilon_1 E_1\left(w^i(t)\right)\right). \tag{3}$$

For $k=1,2,\ldots,K$, the Kth residual component can be calculated as follows:

$$r_k(t) = r_{k-1}(t) - \mathrm{IMF}_k. \tag{4}$$

(3) The white noise $r_1(t)+\varepsilon_1 E_1(\omega^i(t))$, $i=1,2,\ldots,I$, is added to the kth residual component and EMD is performed. Then, IMF_{k+1} can be calculated with the mean value of the first IMF:

$$\mathrm{IMF}_{k+1} = \frac{1}{I}\sum_{i=1}^{I} E_1\left(r_k(t)+\varepsilon_k E_k\left(w^i(t)\right)\right). \tag{5}$$

(4) Repeat equation (4) and (5) until the value of residual component is less than two extremes, and then the decomposition is stopped. Eventually, the residual variable is obtained:

$$r(t) = X(t) - \sum_{k=1}^{K}\mathrm{IMF}_k, \tag{6}$$

where K is the total number of modes in the decomposition process, and the reconstructed signal can be expressed as follows:

$$X(t) = r(t) + \sum_{k=1}^{K}\mathrm{IMF}_k. \tag{7}$$

2.1.2. Selection of IMFs. The raw signal is transformed to a series of IMFs via CEEMDAN, but not all IMFs are related to fault. Some IMFs contain few fault information; thus, these IMFs have no contribution to the following fault identification but do impact the analysis speed. We must therefore develop an IMF selection methodology for selecting the better sensitive IMF related to fault.

The parameter correlation coefficient with time can show the related degree between two signals. According to the Schwarz inequality, we can see the following: $\rho_{xy}(\tau)>0$ represents positive correlation, $\rho_{xy}(\tau)<0$ represents negative correlation, $\rho_{xy}(\tau)=0$ represents no correlation, $\rho_{xy}(\tau)=1$ represents perfectly positive correlation, and $\rho_{xy}(\tau)=-1$ represents perfectly negative correlation, where $\rho_{xy}(\tau)$ is the correlation coefficient. The greater the absolute value of $\rho_{xy}(\tau)$ is, the higher the related degree will be.

This paper proposes the selection of effective IMFs according to the correlation coefficient of the raw signal and each IMF. The IMFs with a higher correlation coefficient, where $|\rho_{xy}(\tau)|\geq 0.6$ represents greater amounts fault information included [24], are selected as the optimal IMFs for the following analysis.

2.2. Permutation Entropy and Its Parameter Selection

2.2.1. The Theory of Permutation Entropy. Entropy can be used to describe the uncertainty of data information. Permutation entropy is a random time sequence detection

method and can reflect the one-dimensional time-series complexity, which has the advantages of simple design, strong antinoise ability, and high robustness. The following are the specific principles of the permutation entropy algorithm.

Assuming a time series $\{a(i),\ i = 1, 2, \ldots, N\}$ with length N, the phase space reconstruction is carried out as follows:

$$H = \begin{bmatrix} H(1) \\ H(2) \\ \vdots \\ H(j) \\ \vdots \\ H(Q) \end{bmatrix} = \begin{bmatrix} a(1)a(1+t) & \cdots & a(1+(m-1)t) \\ a(2)a(2+t) & \cdots & a(2+(m-1)t) \\ \cdots & \cdots & \cdots \\ a(j)a(j+t) & \cdots & a(j+(m-1)t) \\ \cdots & \cdots & \cdots \\ a(Q)a(Q+t) & \cdots & a(Q+(m-1)t) \end{bmatrix}, \tag{8}$$

where $j = 1, 2, 3, \ldots, Q$, m is the embedded dimension, t is the delay time, and $Q + (m-1)t = n$. Next, rearrange the jth component of refactoring matrix in ascending order, so that

$$H(j) = \{a(j+(i_1-1)t) \le a(j+(i_2-1)t) \le \cdots \le a(j+(i_m-1)t)\}, \tag{9}$$

where $i_1, i_2, \ldots, i_m$ is the column position of $H(j)$. If $a(j+(i_e-1)t) = a(j+(i_c-1)t)$ exists, they are arranged by the values of **e** and **c**, while if $e > c$, $a(j+(i_e-1)t) \ge a(j+(i_c-1)t)$ and vice versa. Therefore, any component $H(j)$ of the reconstructed matrix H can be used to obtain the corresponding position sequence:

$$S(j) = (i_1, i_2, \ldots, i_m), \quad j = 1, 2, 3, \ldots, q, \tag{10}$$

where $q \le m!$; due to m different codes $[i_1, i_2, \ldots, i_m]$, there are $m!$ different permutations, namely, $m!$ different symbol sequences. $S(j)$ is just one of the $m!$ code sequences.

Next, calculate the probability of each sequence $P_1, P_2, \ldots, P_q$, $\sum_{j=1}^{q} P_j = 1$. The permutation entropy of the signal time series $\{a(i),\ i = 1, 2, \ldots, N\}$ can be defined in the *Shannon* entropy form as follows:

$$L_{\mathrm{PE}}(m) = -\sum_{j=1}^{q} P_j \ln P_j. \tag{11}$$

When $P_j = 1/m$, $L_{PE}(m)$ will maximize $\ln(m!)$. Then, use $\ln(m!)$ to standardize the permutation entropy $L_{\mathrm{PE}}(m)$:

$$L_{\mathrm{PE}} = \frac{L_{\mathrm{PE}}(m)}{\ln(m!)}, \tag{12}$$

where $0 \le L_{\mathrm{PE}} \le 1$. The value of L_{PE} represents the degree of randomness of the one-dimensional time series. When L_{PE} is larger, the randomness of the time series is stronger. On the contrary, this indicates that the regularity of the time series is stronger.

2.2.2. Calculation of Parameters Selection. In the permutation entropy calculation process, there are two important parameters, namely, the embedded dimension m and the delay time t, where the different settings of these two parameters will have an impact on the calculation results. Selecting the proper embedding dimension m and time delay t is the key to extracting the permutation entropy feature of spiral-bevel gears.

By comparing the original vibration signals of spiral-bevel gears with different fault states, and combining with an analysis of existing literature, it is observed that the embedded dimension $m = 4, 5, 6$ and time delay $t = 1, 2, 3$ are more suitable to the slight mutation of vibration signals, and then the optimal parameters are selected from these values. Due to the fact that embedding dimension and delay together impacts the calculation results, it is not reasonable to consider the change of a single parameter. In this paper, the overlapping grouping method is adapted to optimally select the embedding dimension and time delay, meaning that a section of original vibration signal of the spiral-bevel gear is divided into a series of subsequences $w_1, w_2, \ldots, w_n$ according to the time series, where w_1 moves back one data point to obtain w_2, and so on. Then, the permutation entropy is calculated by the combination of embedded dimension and time delay. Since larger w cannot accurately reflect the signal changes and smaller w has low efficiency and no statistical significance, $w = 128$ is selected.

Figure 1 shows the combination of the original vibration signals in the normal state and the 2/3 broken tooth fault state of the spiral-bevel gear with a sampling frequency of 16384 Hz, where 0-1 s is the normal gear state, and 1-2 s is the two-third broken tooth state.

Figure 2(a) shows the calculation values of permutation entropy when $t = 1$ and $m = 4, 5$, and 6. Figure 2(b) shows the calculation values of permutation entropy when $t = 2$ and $m = 4, 5$, and 6. Figure 2(c) shows the calculation values of permutation entropy when $t = 3$ and $m = 4, 5$, and 6.

It can be seen from Figure 2 that the permutation entropy under the normal state is larger than that under the 2/3 broken tooth fault states. This is because the vibration signal of the spiral-bevel gear under normal states is more random, and when the tooth appears to be broken, it will result in regular shock signals, and thus the vibration under 2/3 broken tooth fault states is more regular. Comparing Figures 2(a), 2(b), and 2(c), it can be found that when $t = 1$ and 2 and $m = 4$ and 5, all permutation entropies can amplify weak information mutation and distinguish normal states and 2/3 broken states, and when $t = 1$ and $m = 4$, the permutation entropy mutation is more obvious when the states undergo mutation. Therefore, the time delay $t = 1$ and embedded dimension $m = 4$ are selected for the following permutation entropy calculation in this paper.

2.3. Sensibility Assessment for CEEMDAN-Based Permutation Entropy. At present, fault diagnosis can be realized by two procedures, namely, feature extraction and mode recognition. Both the sensitivity of features and effectiveness of the classifiers determine the diagnostic accuracy. By selecting the same classification and different feature

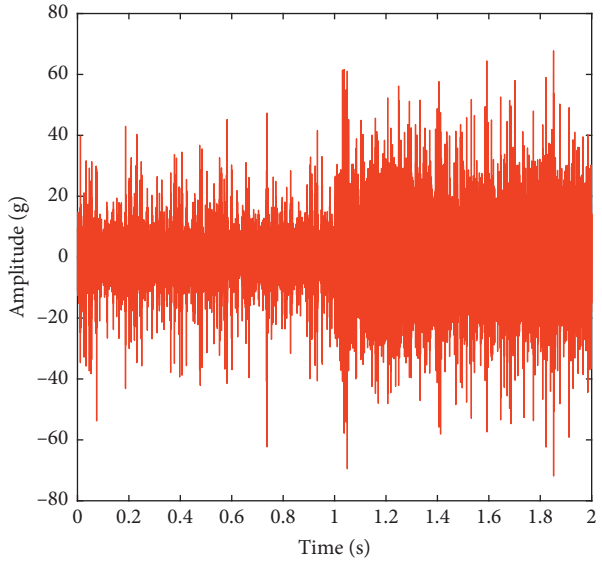

Figure 1: Normal state and 2/3 broken tooth state vibration signal combination.

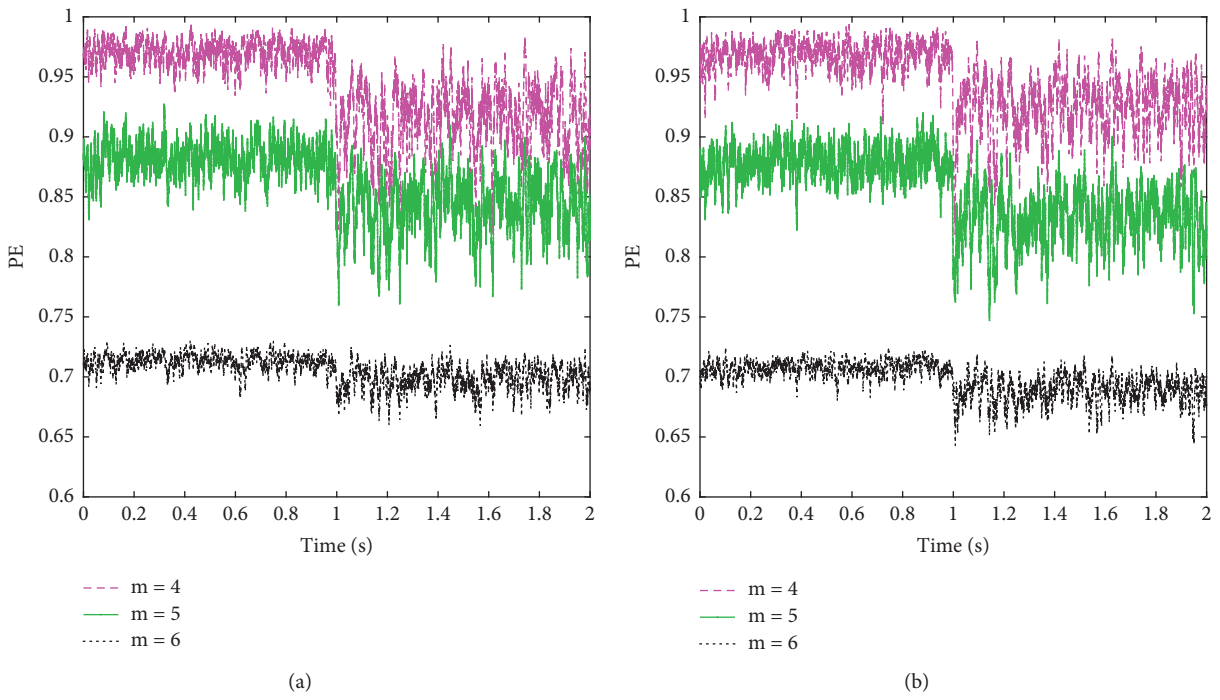

Figure 2: Continued.

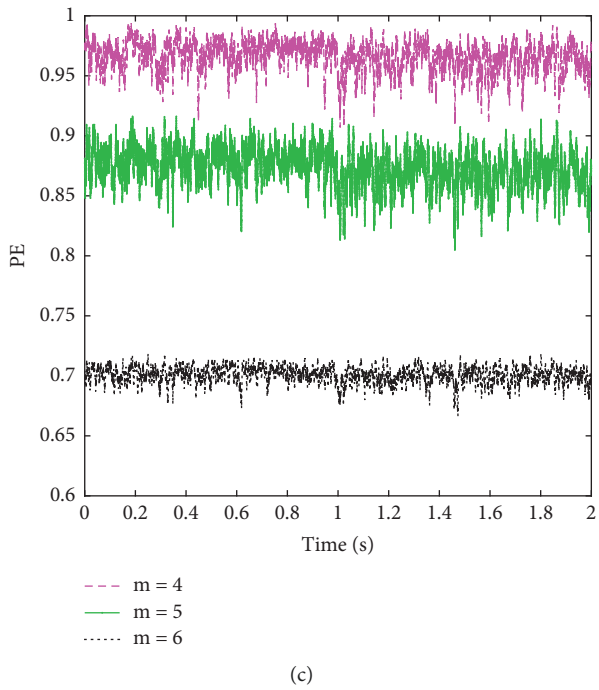

(c)

Figure 2: The calculation values of permutation entropy with different m and t. (a) $t = 1$ and $m = 4$, 5, and 6. (b) $t = 2$ and $m = 4$, 5, and 6. (c) $t = 3$ and $m = 4$, 5, and 6.

vectors, the final diagnostic accuracy can reflect the sensitivity of the features. Based on this ideology, the SVM is used as the classifier for mode recognition, and the final diagnostic accuracy is used to assess the sensibility of CEEMDAN-based permutation entropy in this paper.

At present, the analysis procedure of this paper is carried out as follows:

(1) Original vibration signal acquisition: the vibration signals of spiral-bevel gears under different typical fault states are collected as the raw time-series signals for subsequent analysis.

(2) CEEMDAN: a series of IMFs are obtained by CEEMDAN of the raw vibration signals under different failure states.

(3) Effective IMFs selected: the correlation coefficient of raw signal and IMF is calculated and is combined with the signal-to-noise ratio value. The IMFs' larger correlation coefficient and high signal-to-noise ratio value are selected for subsequent analysis.

(4) Permutation entropy calculation: the permutation entropy of the optimal IMFs is calculated using the time delay $t = 1$ and embedded dimension $m = 4$, and then the multidimensional eigenvector $[L_{PE1}, L_{PE2}, \ldots, L_{PEh}]$ is constructed.

(5) SVM classifier for mode recognition: the characteristic vector obtained in Step (4) is used to train and test the SVM and obtain diagnostic accuracy.

(6) Sensibility assessment: the accuracy of CEEMDAN-based permutation entropy is verified based on the diagnostic accuracy.

3. Experimental Setup and Data Acquisition

The experimental data are collected to evaluate the effectiveness of the method presented in this paper. The spiral-bevel gearbox test equipment used for vibration signal acquisition under typical fault states is shown in Figure 3. The test equipment is composed of a governor, a motor, a coupling, a pair of spiral-bevel gears, and a load. The respective numbers of driving gears and driven gears are 10 and 30. The driving gear is used as the test gear to simulate three typical fault gears, normal tooth, 1/3 broken tooth, and 2/3 broken tooth, respectively, as shown in Figure 4. The accelerometers were placed at three positions: one at the input shaft support bearing, one at the output shaft support bearing, and one at the top of the gearbox. The vibration signals are collected by using B&K's PULSE data acquisition system. During the test, the speed of the motor is kept constant by adjusting the governor to 1200 r/min, and the vibration signals with three different degrees of broken teeth and the same load are collected three times at each mode. The sampling frequency is 16384 Hz.

The time-domain vibration signals under three states of spiral-bevel gears are shown in Figure 5. It can be seen from Figure 5 that the vibration signal under the normal state shown in Figure 5(a) is relatively scattered. The 1/3 broken

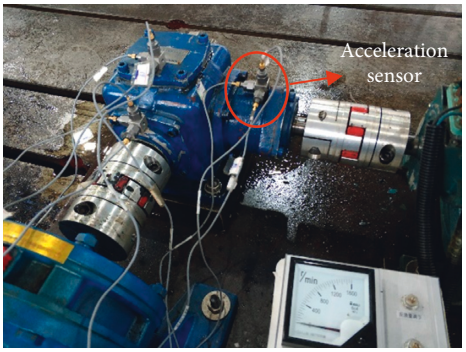

Figure 3: Spiral-bevel gearbox test equipment.

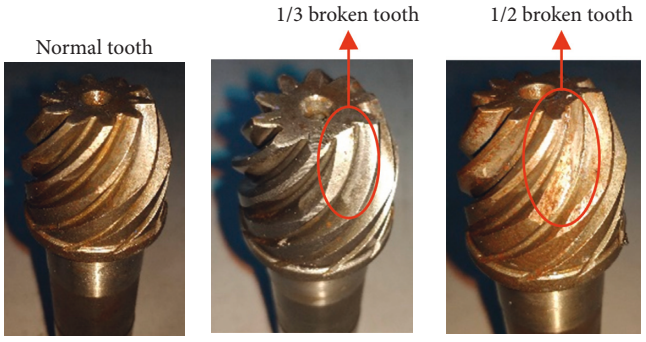

Figure 4: Gears with different degrees of broken teeth.

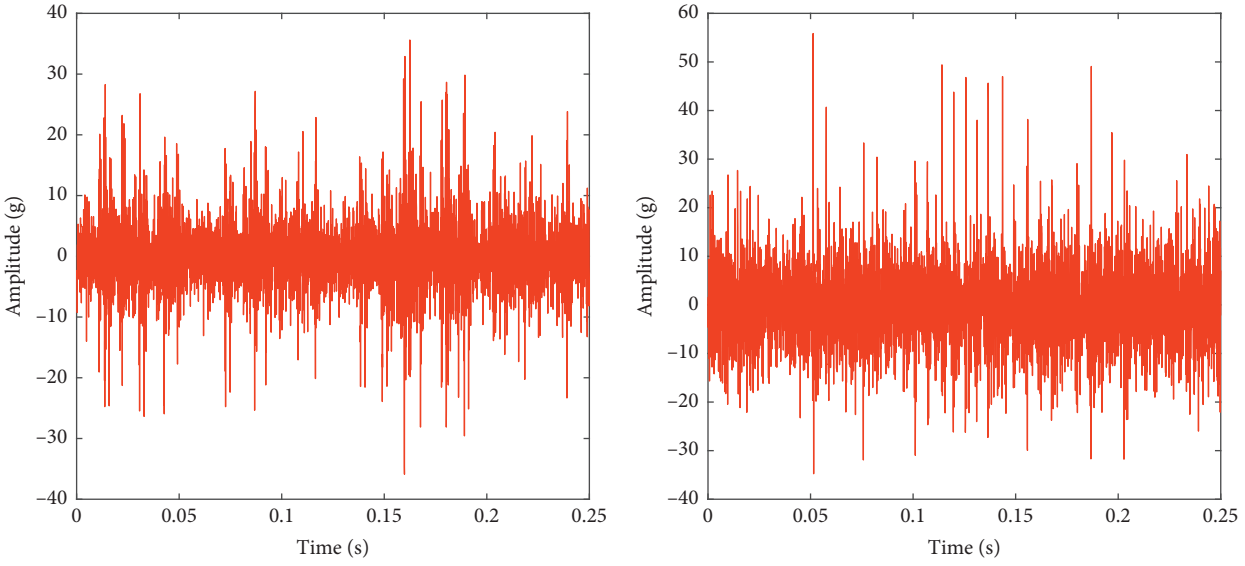

Figure 5: Continued.

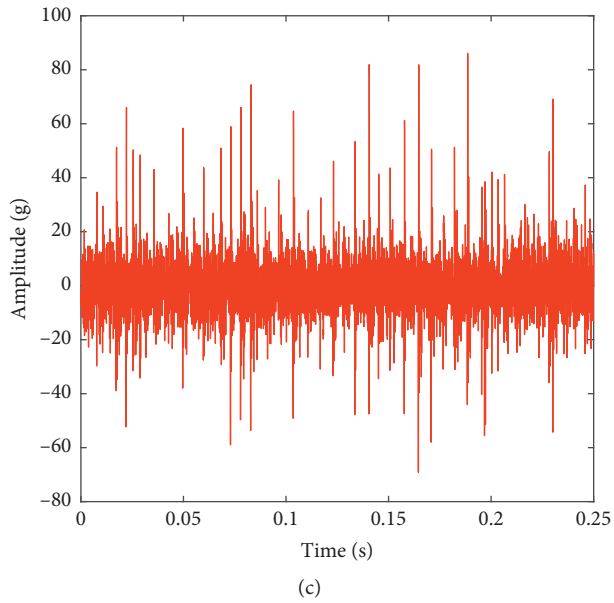

Figure 5: The time-domain vibration signals under three states of spiral-bevel gears. (a) Normal tooth. (b) 1/3 broken tooth. (c) 2/3 broken tooth.

tooth state and 2/3 broken tooth state shown in Figures 5(b) and 5(c) show that the amplitude peak value increases significantly compared with the normal state, and as the degree of broken tooth increases, the vibration impact of tooth engagement becomes greater.

The axial vibration signals from the input shaft support bearing are divided into segments and then processed according to the method described in Section 2.

4. Results and Discussion

The raw vibration signals of the spiral-bevel gear under three failure states are decomposed by the CEEMDAN method, in which the noise standard deviation of CEEMDAN is 0.19, and the overall average frequency is 100. Due to space limitations, only the CEEMDAN results of the 1/3 broken tooth are shown in Figure 6. It can be seen from the figure that the original vibration signal is decomposed into 13 IMFs, of which the 13th component is the residual term. The mode-mixing phenomenon of the waveform gradually weakens from IMF_1 to IMF_{12}, and the frequency is also distributed from high to low.

The correlation coefficients and signal-to-noise ratio of each IMF shown in Figure 6 are calculated, and the results are shown in Table 1. It can be seen from Table 1 that the first two orders of IMFs are highly correlated with the raw vibration signal, both being above 0.6; thus, the first two orders of IMFs are selected.

The permutation entropy of the first two IMFs under three failure states is calculated with time delay $t = 1$ and embedded dimension $m = 4$. The comparison diagram of three failure states is shown in Figure 7. From Figure 7, it can be seen that the permutation entropy of the optimally selected IMFs can clearly distinguish among three typical failure states of spiral-bevel gears.

In order to further verify the sensitivity of CEEMDAN-based permutation entropy, the permutation entropies of IMF_1 and IMF_2 are used to construct a two-dimensional feature vector, then the SVM is used to classify the mode recognition, and the final diagnostic accuracy is used to assess the sensibility of CEEMDAN-based permutation entropy. With 40 samples of each fault state, a total of 120 samples are used as the training samples. The normal state label of spiral-bevel gears is set as "1," the state of 1/3 broken tooth is set as "2," and that of 2/3 broken tooth is set as "3." The RBF Gaussian kernel radial basis function is used for the SVM kernel function, and the grid search method of cross validation is used to determine the optimal penalty factor and kernel function parameters. With 40 samples of each fault state, a total of 120 samples are used as the test samples and input into the trained SVM classifier for classification and recognition. The classification results are shown in Figure 8, with an accuracy rate of 100%, which indicates that the CEEMDAN-based permutation entropy has a high sensitivity for fault identification in spiral-bevel gears.

In order to verify the superiority of CEEMDAN-based permutation entropy, we compare it with EEMD-based permutation entropy. The same vibration signals of the spiral-bevel gear in the aforementioned results are decomposed by the EEMD method, and the permutation entropy values of the first two IMFs are calculated with the same parameter set. The comparison diagram of EEMD-based

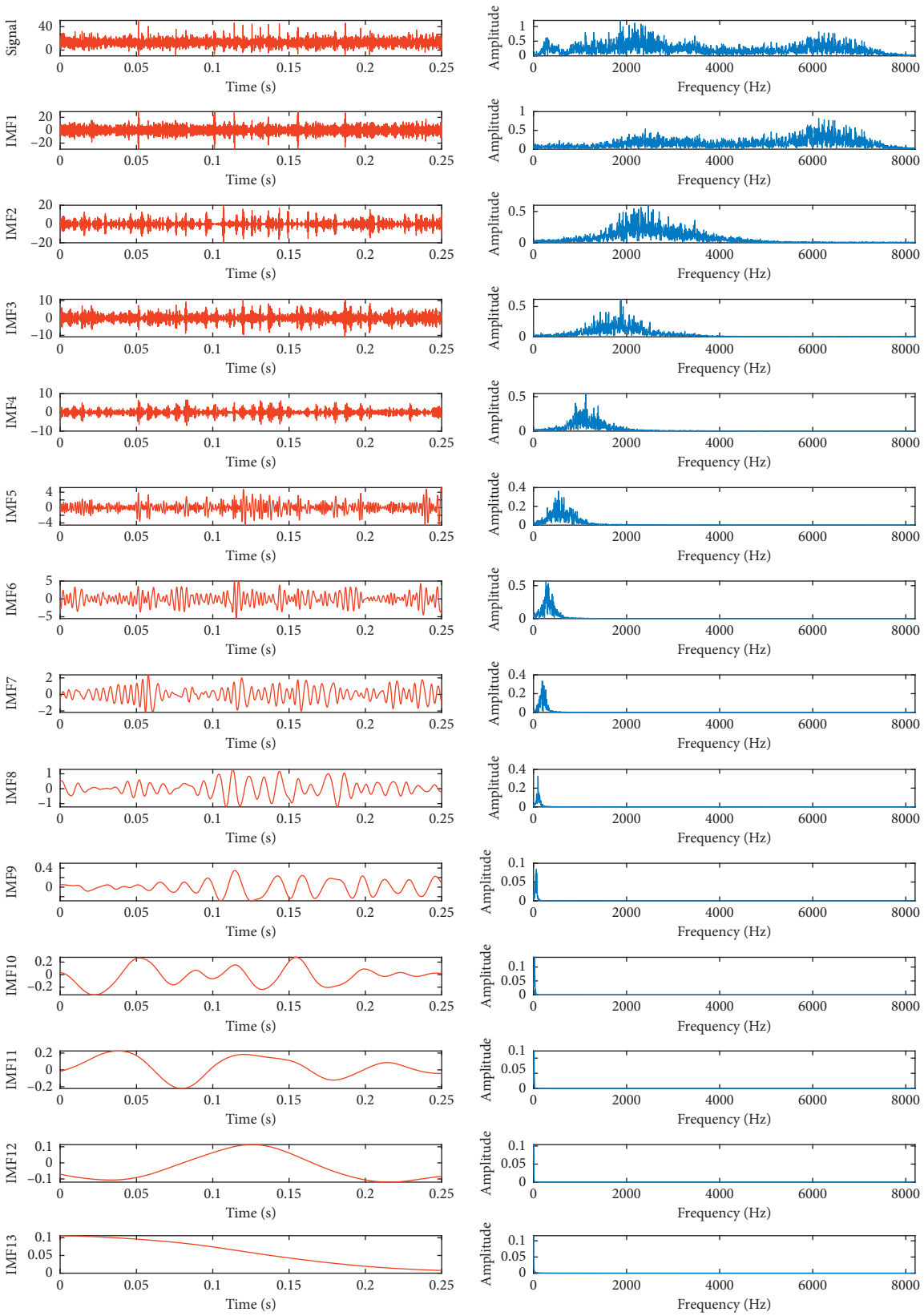

Figure 6: CEEMDAN results.

Table 1: Correlation coefficient.

IMF component	Correlation coefficient
IMF_1	0.731
IMF_2	0.634
IMF_3	0.506
IMF_4	0.292
IMF_5	0.176
IMF_6	0.184
IMF_7	0.079
IMF_8	0.013
IMF_9	0.0031
IMF_{10}	0.0059
IMF_{11}	0.0035
IMF_{12}	−8.68e-04
IMF_{13}	7.35e-04

permutation entropy of the three failure states is shown in Figure 9. It can be seen that the permutation entropy of the optimal selected IMFs of EEMD can distinguish three typical failure states of the spiral-bevel gear, but the distinction ability is not as good as the CEEMDAN-based method. The reason for this is that the resulting IMFs derived from the EEMD method would inevitably be contaminated by the added noise, especially when the number of ensembles is relatively low.

The two-dimensional feature vectors constructed by EEMD-based permutation entropy are input into the SVM classifier for training and testing. The test results are shown in Figure 10. From Figure 10, it can be seen that the overall classification result is only 88.33%. In addition, for label "1," i.e., the normal state of the spiral-bevel gear, 7 of the 40 test samples are incorrectly identified, and for label "2," i.e., one-third of the broken tooth, 7 of the 40 test samples are also incorrectly identified, while for label "3," i.e., two-third of the broken tooth, the identification results are completely accurate.

As discussed earlier, the two-dimensional feature vectors constructed by EMD-based permutation entropy are input into the SVM classifier for training and testing. The test results are shown in Figure 11, where it can be seen that the overall classification result is only 83.33%. For label "1," i.e., the normal state of the spiral-bevel gear, 5 of the 40 test samples are incorrectly identified, and for label "2," i.e., one-third of the broken tooth, 5 of the 40 test samples are also incorrectly identified, while for label "3," i.e., two-third of the broken tooth, 10 of the 40 test samples are incorrectly identified. The reason for this is that EMD has the major drawback of mode mixing.

As illustrated in Section 2.3, which features the same classification tool but different feature vectors for the fault mode recognition of spiral-bevel gears, the diagnostic accuracy can reflect the sensitivity of the features. Therefore, compared with the diagnostic results by using CEEMDAN-based/EEMD-based/EMD-based permutation entropy and SVM, it is easy to reach a conclusion, and the CEEMDAN-based permutation entropy is the most sensitive feature for fault identification of spiral-bevel gears.

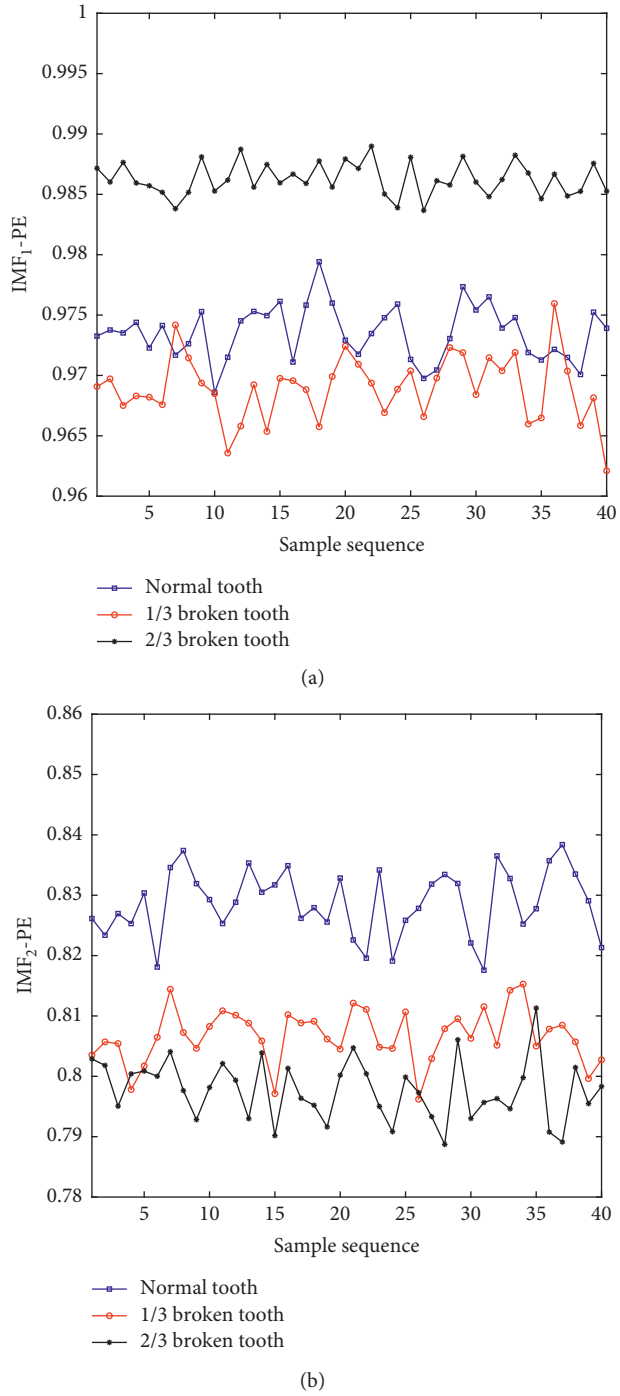

Figure 7: Comparison of CEEMDAN-based permutation entropy of three states. (a) Permutation entropy of IMF_1. (b) Permutation entropy of IMF_1.

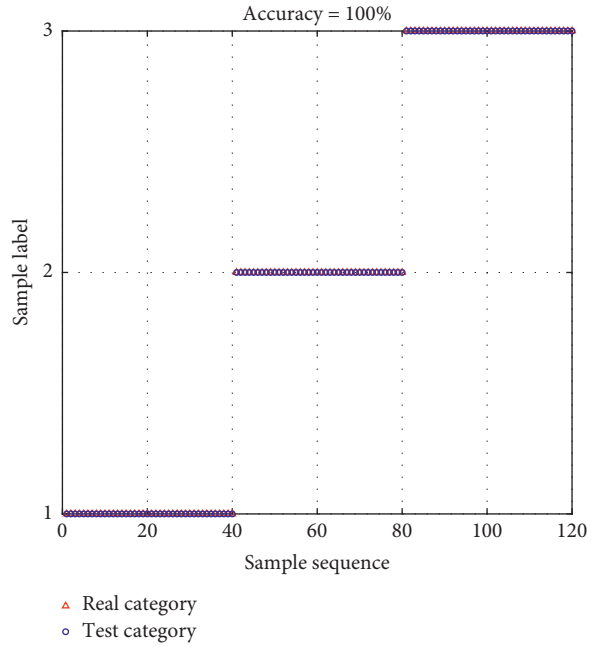

Figure 8: The spiral-bevel gear fault diagnostic results by using CEEMDAN-based permutation entropy and SVM.

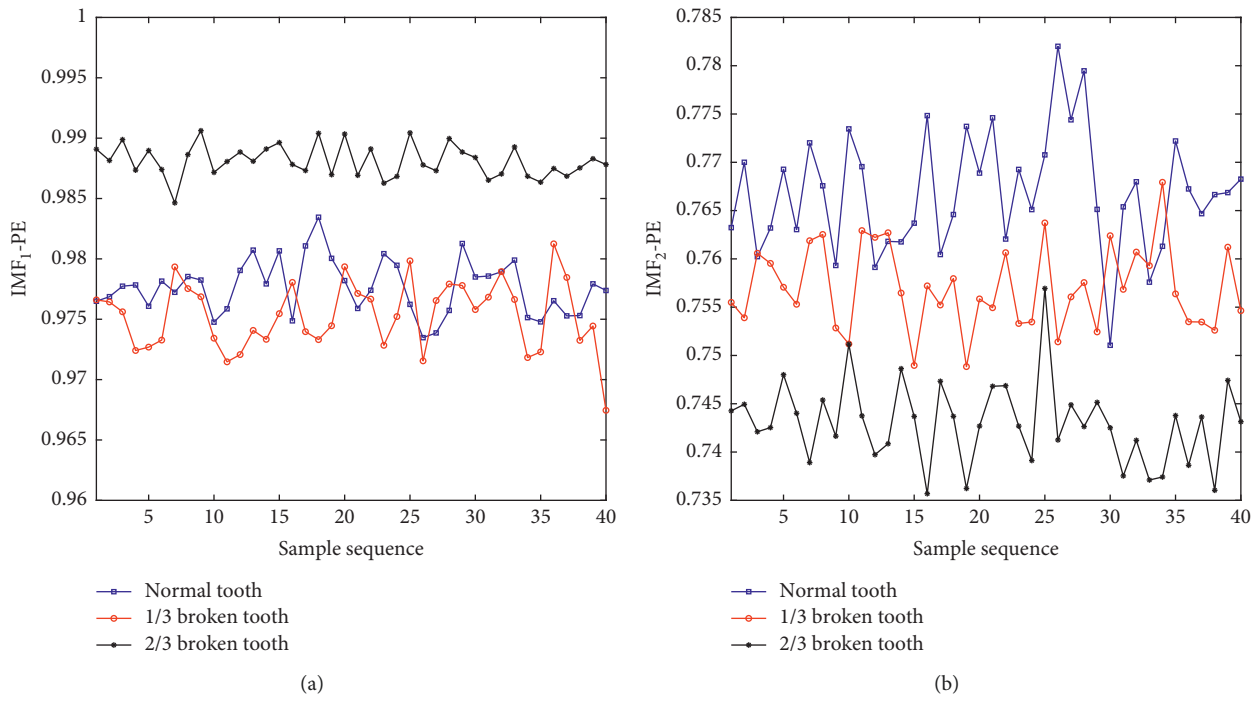

Figure 9: Comparison of EEMD-based permutation entropy of three states. (a) Permutation entropy of IMF_1. (b) Permutation entropy of IMF_2.

5. Conclusion

This paper proposes to take the CEEMDAN-based permutation entropy as the sensitive feature for fault identification of spiral-bevel gears. An experimental study has been carried out on a spiral-bevel gearbox to verify the effectiveness of the feature. From observations of the analytical results, the following conclusions are drawn:

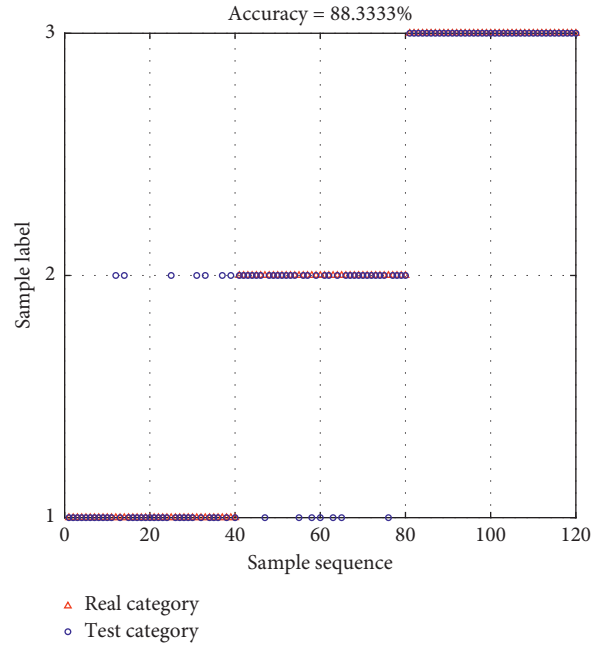

Figure 10: The spiral-bevel gear fault diagnostic results by using EEMD-based permutation entropy and SVM.

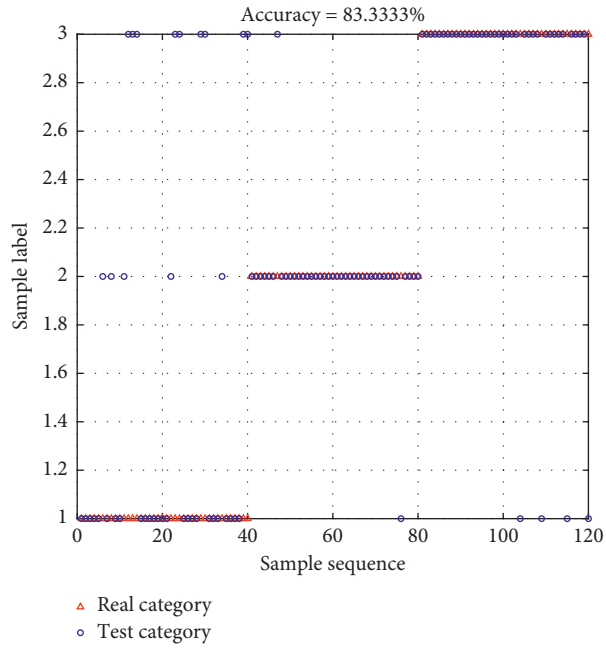

Figure 11: The spiral-bevel gear fault diagnostic results by using EMD-based permutation entropy and SVM.

(1) The CEEMDAN-based permutation entropy of the first two IMFs can be used to clearly distinguish three typical failure states of spiral-bevel gears.

(2) Using the CEEMDAN-based permutation entropy to construct the feature vector and the SVM as the classifier for fault mode recognition of the spiral-bevel gears, the accuracy of the high spiral-bevel gears fault diagnostic verifies the sensitivity of the feature.

(3) Compared with the diagnostic results based on CEEMDAN-based/EEMD-based/EMD-based permutation entropy and SVM, the diagnostic accuracies are 100%, 88.33%, and 83.33%, respectively, which indicates that the CEEMDAN-based permutation entropy is the most sensitive feature for fault identification of spiral-bevel gears.

In this paper, the sensitive feature is used to analyze the fault mode of spiral-bevel gears. Our future research will focus on the analysis of the fault severity.

Data Availability

The data used to support the findings of this study are available from the corresponding author upon request.

Conflicts of Interest

The authors declare that they have no conflicts of interest.

Acknowledgments

This study was supported by the National Natural Science Foundation of China (grant nos. 51575177 and 11872022) and the Outstanding Youth Program of Hunan (grant no. 2017RS3049).

References

[1] T. Wang, X. Wu, T. Liu et al., "Gearbox fault detection and diagnosis based on EEMD de-noising and power spectrum," in *Proceedings of the IEEE International Conference on Information &Automation*, pp. 1528–1531, IEEE, Lijiang, China, August 2015.

[2] V. Sharma and P. Anand, "Case study on the effectiveness of gear fault diagnosis technique for gear tooth defects under fluctuating speed," *IET Renewable Power Generation*, vol. 11, no. 14, pp. 1841–1849, 2017.

[3] M. Buzzoni, G. D'Elia, E. Mucchi, G. Dalpiaz, and E. Mucchi, "A vibration-based method for contact pattern assessment in straight bevel gears," *Mechanical Systems and Signal Processing*, vol. 120, pp. 693–707, 2019.

[4] N. Saravanan and K. I. Ramachandran, "Incipient gear box fault diagnosis using discrete wavelet transform (DWT) for feature extraction and classification using artificial neural network (ANN)," *Expert Systems with Applications*, vol. 37, no. 6, pp. 4168–4181, 2010.

[5] S. He, Y. Zi, Z. Wan et al., "Application of adaptive multi-wavelets via lifting scheme in bevel gear fault diagnosis," *Chinese Journal of Scientific Instrument*, vol. 35, no. 1, pp. 148–153, 2014, in Chinese.

[6] S. Kumar, D. Goyal, R. K. Dang, S. S. Dhami, and B. S. Pabla, "Condition based maintenance of bearings and gears for fault detection—a review," *Materials Today: Proceedings*, vol. 5, no. 2, pp. 6128–6137, 2018.

[7] Y. Lei, J. Lin, M. J. Zuo, and Z. He, "Condition monitoring and fault diagnosis of planetary gearboxes: a review," *Measurement*, vol. 48, pp. 292–305, 2014.

[8] Y. Chen, T. Zhang, Z. Luo, and K. Sun, "A novel rolling bearing fault diagnosis and severity analysis method," *Applied Science*, vol. 9, p. 2356, 2019.

[9] Y. Lei, J. Lin, Z. He, and M. J. Zuo, "A review on empirical mode decomposition in fault diagnosis of rotating machinery," *Mechanical Systems and Signal*, vol. 35, no. 1-2, pp. 108–126, 2013.

[10] A. Mejia-Barron, M. Valtierra-Rodriguez, D. Granados-Lieberman, J. C. Olivares-Galvan, and R. Escarela-Perez, "The application of EMD-based methods for diagnosis of winding faults in a transformer using transient and steady state currents," *Measurement*, vol. 117, pp. 371–379, 2018.

[11] Z. Wu and N. E. Huang, "Ensemble empirical mode decomposition: a noise-assisted data analysis method," *Advances in Adaptive Data Analysis*, vol. 1, no. 1, pp. 1–41, 2009.

[12] J.-R. Yeh, J.-S. Shieh, and N. E. Huang, "Complementary ensemble empirical mode decomposition: a novel noise enhanced data analysis method," *Advances in Adaptive Data Analysis*, vol. 2, no. 2, pp. 135–156, 2010.

[13] M. E. Torres, M. A. Colominas, G. Schlotthauer, and P. Flandrin, "A complete ensemble empirical mode decomposition with adaptive noise," in *Proceedings of the IEEE International Conference on Acoustics, Speech and Signal Processing*, pp. 4144–4147, IEEE, Prague, Czech Republic, May 2011.

[14] Vanraj, S. S. Dhami, and B. S. Pabla, "Non-contact incipient fault diagnosis method of fixed-axis gearbox based on CEEMDAN," *Royal Society Open Science*, vol. 4, no. 8, Article ID 170616, 2017.

[15] M. Kuai, G. Cheng, Y. Pang, and Y. Li, "Research of planetary gear fault diagnosis based on permutation entropy of CEEMDAN and ANFIS," *Sensors*, vol. 18, no. 3, pp. 1–17, 2018.

[16] J. B. Ali, N. Fnaiech, L. Saidi, B. Chebel-Morello, and F. Fnaiech, "Application of empirical mode decomposition and artificial neural network for automatic bearing fault diagnosis based on vibration signals," *Applied Acoustics*, vol. 89, pp. 16–27, 2015.

[17] S. Hong, Z. Zhou, E. Zio, and K. Hong, "Condition assessment for the performance degradation of bearing based on a combinatorial feature extraction method," *Digital Signal Processing*, vol. 27, pp. 159–166, 2014.

[18] H. Xu and G. Chen, "An intelligent fault identification method of rolling bearings based on LSSVM optimized by improved PSO," *Mechanical Systems and Signal Processing*, vol. 35, no. 1-2, pp. 167–175, 2013.

[19] C. Bandt and B. Pompe, "Permutation entropy: a natural complexity measure for time series," *Physical Review Letters the American Physiological Society*, vol. 88, no. 17, Article ID 174102, 2002.

[20] X. Zhang, Y. Liang, J. Zhou, and Y. Zang, "A novel bearing fault diagnosis model integrated permutation entropy, ensemble empirical mode decomposition and optimized SVM, ensemble empirical mode decomposition and optimized SVM," *Measurement*, vol. 69, pp. 164–179, 2015.

[21] Z. Shi, W. Song, and S. Taheri, "Improved LMD, permutation entropy and optimized K-means to fault diagnosis for roller bearings," *Entropy*, vol. 18, no. 3, p. 70, 2016.

[22] C. Ding, B. Zhang, F. Feng, and P. Jiang, "Application of local mean decomposition and permutation entropy in fault diagnosis of planetary gearboxes," *Journal of Vibration and Shock*, vol. 36, no. 17, pp. 55–60, 2017, in Chinese.

[23] J. D. Zheng, J. S. Cheng, and Y. Yang, "Multiscale permutation entropy based rolling bearing fault diagnosis," *Shock and Vibration*, vol. 2014, Article ID 154291, 8 pages, 2014.

[24] L. L. Jiang, Y. L. Liu, X. J. Li, and D. L. Yang, "Feature extraction of weak signal using wavelet packet denoising and improved hillbert-huang transformation," *Journal of Vibration, Measurement & Diagnosis*, vol. 30, no. 5, pp. 510–513, 2010, in Chinese.